Double charge exchange in $^{93}Nb(\pi^+, \pi^-)^{93}Tc$ at $T_\pi = 164$, 230, and 294 MeV

M. A. Kagarlis*
University of Pennsylvania, Philadelphia, Pennsylvania 19104
and Los Alamos National Laboratory, Los Alamos, New Mexico 87545

H. T. Fortune, P. Hui, S. Loe, D. A. Smith, and A. L. Williams
University of Pennsylvania, Philadelphia, Pennsylvania 19104

J. Urbina
New Mexico State University, Las Cruces, New Mexico 88003
(Received 3 September 1992)

In pion-induced double charge exchange on ^{93}Nb, a number of new discrete states, in addition to the ground state and the double isobaric analog state (DIAS), have been observed in the residual ^{93}Tc nucleus. Cross sections for the different states exhibit widely different energy dependence characteristics. In particular, the state just below the DIAS has a very different excitation function from the DIAS. In addition, the cross section of the giant resonance GDR⊗IAS has been measured at $T_\pi = 230$ and 294 MeV.

PACS number(s): 25.80.Gn, 27.60.+j

I. INTRODUCTION

The present paper describes a double charge exchange (DCX) experiment, a study of the reaction $^{93}Nb(\pi^+, \pi^-)^{93}Tc$ at a scattering angle of 5° and three laboratory beam energies, $T_\pi = 164$, 230, and 293.7 MeV. The experiment ran at the EPICS (Energetic Pion Channel and Spectrometer) channel of the Los Alamos Meson Physics Facility (LAMPF). The motivation was the earlier accidental observation of a certain class of states, which became known in the literature as the $T_<$ (T-lower) states, in DCX experiments on ^{93}Nb, ^{56}Fe, and ^{138}Ba at 295 MeV [1–3]. The experiments which used ^{56}Fe and ^{138}Ba were aiming to measure the DIAS; although it was possible to resolve the $T_<$ states, the statistics were poor. The experiment that used ^{93}Nb was designed to study giant resonances of excitation energies much higher than the $T_<$ states, and had the focal plane of the EPICS spectrometer set so that the $T_<$ states were barely admissible at the edge of its acceptance. Thus more careful measurements of the $T_<$ states were in order.

Although the large volume of DCX measurements for transitions to the double isobaric analog state (DIAS) and to the ground state (g.s.) of the residual nuclei has allowed for a detailed study of the mechanisms by which these states are populated, such information was unavailable for the $T_<$ states. Thus, from the preliminary measurements of the $T_<$ states, two questions arose: (a) whether $T_<$ states are a common characteristic of heavy nuclei, and (b) what is the DCX mechanism via which the $T_<$ states are populated.

Since the energy dependence of DCX cross sections is one of the signatures of the reaction mechanisms possible in DCX, measurements at more than one laboratory beam energy were necessary for a better understanding of the $T_<$ states. The three energies selected for this experiment, viz., $T_\pi = 164$, 230, and 294 MeV, aim at examining the energy dependence of the $T_<$ states near (164 MeV) and away (294 MeV) from the Δ_{33} resonance, as well as at some intermediate energy (230 MeV). Away from the Δ_{33} resonance the dominant DCX mechanism is believed to be sequential scattering of the projectile pion from two nucleons with eventual exchange of two units of charge [4], while at resonance it is believed possible that a resonant excitation of a Δ_{33} in the nucleus is dominant, resulting from the direct interaction of the projectile pion with one nucleon alone coupled with a Δ-nucleon charge exchange (nonsequential) [5–7].

The small DCX cross sections, hampered further by the recent reduction of the time allocated to experimental cycles at LAMPF, make full angular distribution measurements prohibitive. Thus the experiment was set for a scattering angle of 5°, at which DCX transitions of zero total angular momentum transfer ($\Delta J = 0$), such as to the DIAS, are largest.

As it turns out, in addition to observing the discrete states of interest below the DIAS in the residual ^{93}Tc, measurements have also been obtained at $T_\pi = 230$ and 294 MeV for the collective giant dipole resonance (GDR) built on the isobaric analog state (IAS⊗GDR). Though peripheral to our study of the discrete states, this giant resonance merits interest of its own.

II. APPARATUS AND NORMALIZATION PROCEDURES

This experiment used the standard DCX setup at EPICS. Several documents exist which discuss in detail the EPICS channel and the spectrometer [8–10]. Here, we briefly note that electrons are eliminated with a velocity-threshold Cherenkov detector, and muons are

*Present address: Niels Bohr Institute, University of Copenhagen, Blegdamsvej 17, DK2100 Copenhagen, Denmark.

rejected with a series of scintillators alternating with graphite plates and fine tuned with aluminum absorbers. Further muon rejection is necessary at lower beam energies (T_π = 164 MeV), and it is achieved with software gating of time-of-flight measurements from two scintillators placed at the front and rear focal planes—before and after the dipole bending magnets of the spectrometer, respectively. For further details on the apparatus, as well as calibration procedures for the EPICS spectrometer, we refer the reader to the literature referenced above. We do discuss, however, the determination of the beam profile and the absolute normalization of the spectrometer, both procedures which are specific to individual experiments, and necessary in order that actual measurements of yields be turned into cross sections.

The yields (defined as y, in units of μb/sr), are the number of counts normalized by the proton beam toroid scalar (1ACM02), spectrometer acceptance, and the detector efficiencies. Yields differ from cross sections by an additional normalization factor, which amounts to the conversion of beam monitor counts to pions per solid angle subtended by the spectrometer. This additional normalization factor is determined by measuring the yield for a target of known cross section and is specific to a particular polarity and central momentum. We denote the dimensionless momentum of the spectrometer as

$$\delta = \frac{p - p_0}{p_0} , \tag{1}$$

where p_0 is the central momentum of the spectrometer, determined by the field settings, and p is the actual momentum of the pion.

The spectrometer accepts particles up to about $\delta = \pm 8\%$, and the normalization factor must be determined as a function of δ. This is done by moving the focal plane of the spectrometer across the range of momentum acceptance, in effect by setting the fields so as to place a known peak at different δ's.

The target typically chosen for the acceptance measurements is ^{12}C since elastic and inelastic angular distributions for carbon are well known. In particular, in the present experiment, ^{12}C cross sections were measured for a beam energy of 180 MeV.

The acceptance measurements as described determine the variation of the normalization factor as a function of δ. At the central momentum, comparison of the measured yield with the known elastic cross section of ^{1}H in a CH_2 target with areal density of 73.2 mg/cm^2 yielded the absolute normalization. These measurements resulted in the following normalization factors for DCX on ^{93}Nb:

$$\begin{aligned} &\text{at 164 MeV}, \sigma_{\mathrm{DCX}} = y_{\mathrm{DCX}}(1.786 \pm 0.035), \\ &\text{at 230 MeV}, \sigma_{\mathrm{DCX}} = y_{\mathrm{DCX}}(1.177 \pm 0.024), \\ &\text{at 293.7 MeV}, \sigma_{\mathrm{DCX}} = y_{\mathrm{DCX}}(1.164 \pm 0.019), \end{aligned} \tag{2}$$

For the DCX measurements a full ^{93}Nb target (roughly, 15 cm × 20 cm) was used, which contained the entire beam spot. The areal density of the target was 1.749 gm/cm^2, relatively thick to maximize the DCX count rates without compromising the resolution necessary for the states of interest. Elastic scattering cross-section measurements were taken for two δ's at each beam energy for which DCX data were taken, namely, at T_π = 164, 230, and 293.7 MeV, at a scattering angle of 35°. Positive polarity pion beams at EPICS reach currents which are higher by up to a factor of 7 from negative polarity beams [8]. Since elastic cross sections are large, the currents in the front chambers for positive polarity beams would be damaging; thus negative polarity pions were used for the elastic measurements. The two δ's were selected so as to be in the proximity of the DIAS and the g.s. for each of the three beam energies.

These measurements were used in two ways: First, at each beam energy, the elastic peak shape corresponding to the δ of the DIAS was used for fitting the DCX spectrum, since the DIAS δ was closer to the center of the focal plane of the spectrometer as set for the DCX measurements. The full width at half maximum for the elastic peak was 590 keV at T_π = 293.7 MeV, 622 keV at T_π = 230 MeV, and 700 keV at T_π =164 MeV. Second, the ^{93}Nb elastic cross sections along with the ^{1}H elastic and the ^{12}C 4.439- and 9.641-MeV inelastic excitations were used to make a minor correction to the Q values and excitation energies obtained by fitting the raw DCX data. As an indication of the size of the corrections made to the measurements of Q values we note that the ratio of the true to the measured difference of the Q values for the two ^{12}C inelastic excitations mentioned above ($\Delta Q_{\mathrm{true}}/\Delta Q_{\mathrm{expt}}$, where ΔQ_{true} = 9.641–4.439 MeV) is 1.0109±0.0003 at T_π = 293.7 MeV, 1.0105±0.0015 at T_π = 230 MeV, and 1.0115±0.0028 at T_π = 164 MeV.

Let us now describe how these measurements were used for energy calibration. A first correction arises from the offset of the projectile central momentum selected by the channel dipole magnets from what it was set to be for the 293.7 MeV spectrum. In particular, although the channel magnets were set for a beam energy of 292 MeV, it was determined that the actual beam energy was 293.7 MeV, from elastic energy measurements in the spectrometer and correcting for the energy loss in the ^{93}Nb target with calculations of Landau energy loss. The reason for this anomaly is that the dipole magnets which momentum analyze the pions in the channel are known to saturate towards the upper limit of pion beams possible at EPICS (i.e., 300 MeV). This results in the bending of the field, which furthermore stretches beyond the limits of the magnets, with the consequence that faster projectiles are selected. Thus pion beams higher by approximately 1.7 MeV from what they were set to be have typically been observed at EPICS, as the beam energy approaches 300 MeV.

TABLE I. Total energy-scale corrections for the DCX measurements, including the energy loss (Landau) in the target.

T_π (MeV)	ΔE (MeV), function of δ
293.7	(−2.302±0.011) − (0.038±0.001)δ
230	(−1.972±0.038) − (0.031±0.001)δ
164	(−2.237±0.029) − (0.026±0.006)δ

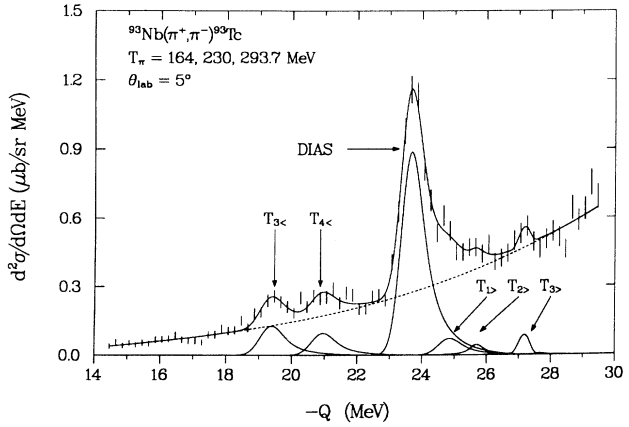

FIG. 1. Spectrum in the region of the DIAS, summed over three beam energies.

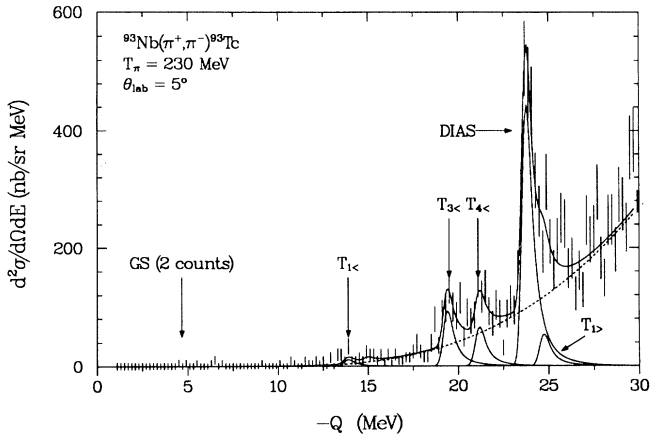

FIG. 3. As in Fig. 2, but for 230 MeV.

Furthermore, we observe that three types of energy scale corrections—this time associated with the spectrometer rather than the channel—are in order, in addition to an overall offset. The origin of the offset may be a one-time effect per measurement, as, for example, the drifting of some fields from their original settings. The remaining corrections result from the dependence of the projectile central momentum on the spectrometer variables, namely, the dipole field δ and the energy gradient with respect to the scattering angle. All these corrections are presumably small, and so their effect will be taken to be linear. We summarize the above assertion in the equation

$$\Delta E_0 + \Delta E_L = \Delta E + \alpha(B - B_0) + \beta(\delta - \delta_0) + \gamma\left(\frac{\partial E}{\partial \theta}\right) , \tag{3}$$

and observe that $\Delta E_0 = E_x - E_{x_0}$ is the difference of the true from the experimental excitation energy for each of the two inelastic excitations in ^{12}C, elastic scattering from ^{1}H, and from ^{93}Nb at two δ's, enumerated earlier. The Landau energy loss ΔE_L and the energy gradient with respect to the scattering angle are calculated. Last, B is the spectrometer dipole field setting which selects the central momentum of the projectiles. We intend to fit for ΔE, α, β, and γ of (3); thus we can afford an arbitrary choice of B_0 and δ_0, since these will be compensated by a readjustment of ΔE. We have used $\delta_0 = 0\%$.

The procedure is the following: First, we fit for the hydrogen elastic peak and the two carbon inelastic excitations simultaneously, for each spectrum. We recall that the hydrogen and carbon measurements were obtained from a single CH_2 target; thus the field settings for the hydrogen and carbon peaks are common. We choose B_0 to be the field setting for ^{1}H and ^{12}C for each spectrum, and δ_0 to be zero. Thus the term which involves α in (3) vanishes for the CH_2 target, and for every spectrum we have a set of three equations in three parameters to be fitted, namely, the equations for the hydrogen elastic peak and the two carbon inelastic excitations, in the parameters ΔE, β, and γ.

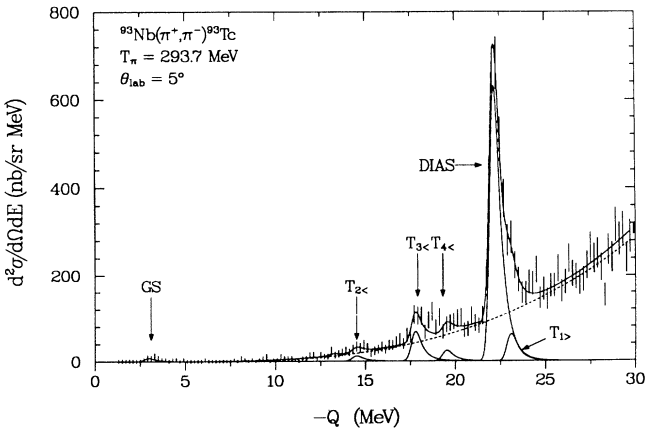

FIG. 2. Spectrum of outgoing pions from ^{93}Nb(π^+,π^-)^{93}Tc at a bombarding energy of 293.7 MeV and a laboratory angle of 5°. Fitting is described in text.

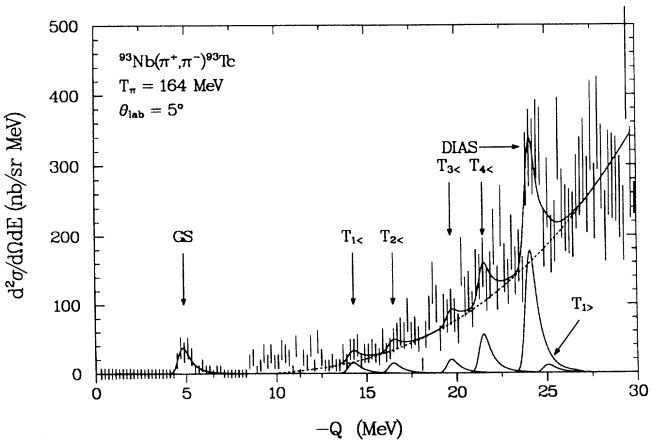

FIG. 4. As in Fig. 2, but for 164 MeV.

While the energy offset ΔE is specific to the CH_2 measurements, the parameters β and γ describe properties of the spectrometer which can be used for the DCX measurements as well. The parameter γ, in particular, was independently determined to be 0.30° at the end of an experiment [11]. Our analysis is consistent with this result at $T_\pi = 293.7$ MeV, and yields $\gamma = 0.27°$ at $T_\pi = 230$ MeV and $\gamma = 0.34°$ at $T_\pi = 164$ MeV. Next, α and ΔE of (3) are fitted to the elastic scattering measurements on ^{93}Nb at two δ's. This analysis yields the total energy corrections to the excitation energies and Q values obtained from our DCX measurements, and are summarized in Table I. We emphasize that these corrections are small, but not negligible. As noted above, they amount to a 1% correction to the Q-value differences.

III. DATA AND ANALYSIS

As we pointed out earlier, some cross sections determined in this experiment had also been measured earlier [1,12]. These are the DIAS, two of the $T_<$ states, and the collective giant resonance GDR⊗IAS at $T_\pi = 292$ MeV. In this experiment data were taken for beam energies of $T_\pi = 164$, 230, and 293.7 MeV. The states observed were those previously measured in addition to the g.s., two more $T_<$ states, and one state above the DIAS (Figs. 1–4). Also, cross sections were measured for the collective giant resonance GDR⊗IAS at beam energies of $T_\pi = 230$ and 293.7 MeV (Fig. 5). The background used for the fits is a third order polynomial in Q, typically used for fitting DCX data. All the states reported here, with the exception of the giant resonance, were fitted with the elastic peak shapes. Attempts to fit the states below and above the DIAS using Lorentzians folded with the elastic peak shapes yielded zero widths, and cross sections as well as χ^2 similar to these obtained by fitting with the elastic peak shapes. For the giant resonance (Fig. 5), a Lorentzian folded with the elastic peak shape was fitted

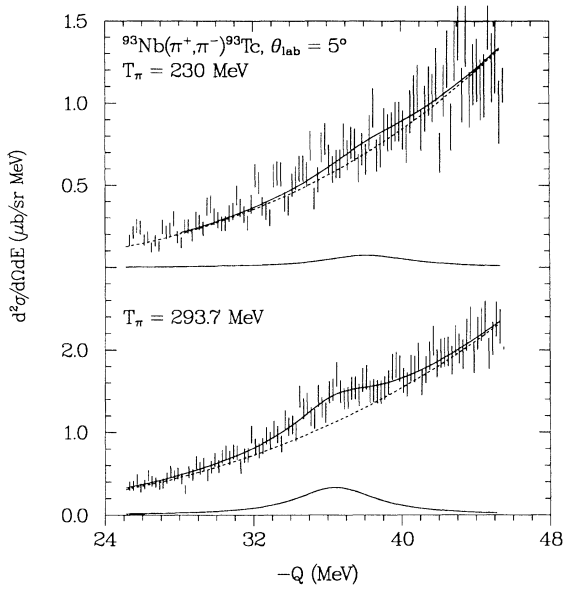

FIG. 5. Region of the GDR⊗IAS at $T_\pi = 293.7$ MeV (bottom) and 230 MeV (top).

for the centroid and width at $T_\pi = 293.7$ MeV. Subsequently, the centroid and width were fixed for the $T_\pi = 230$ MeV spectrum, where the statistics did not allow for an independent determination of these parameters. At $T_\pi = 164$ MeV the giant resonance fell outside of the acceptance of the EPICS spectrometer. In general, the same procedure was used for the discrete states as well: the centroid—there is no width, since the shape was fixed to be the elastic peak shape for all the discrete states—was fitted in the spectrum where the statistics allowed, and subsequently it was fixed in the remaining spectra. When summing the three spectra in the proximity of the

TABLE II. Measurements from present experiment. All DCX data were at a laboratory angle of 5°.

		T_π=164 MeV	T_π=230 MeV	T_π=293.7 MeV
State	$-Q$ (MeV)	$d\sigma/d\Omega$ (nb/sr)	$d\sigma/d\Omega$ (nb/sr)	$d\sigma/d\Omega$ (nb/sr)
g.s.	2.42±0.09[a]	36.4± 4.2	2.2± 1.5	6.0± 2.8
$T_{1<}$	11.96±0.19[b]	15.1± 4.7	10.0± 4.0	
$T_{2<}$	14.21±0.19[c]	14.1± 5.8		10.3± 4.6
$T_{3<}$	17.50±0.07[d]	18.7± 7.9	82.8± 11.0	64.5± 9.1
$T_{4<}$	19.28±0.09[d]	52.3±10.2	59.9± 12.0	26.0± 8.9
DIAS	21.95±0.02[c]	166.4±15.7	400.6± 24.8	511.7± 21.5
$T_{1>}$	22.90±0.11[c]	11.2±13.8	48.7± 17.6	53.5± 13.5
GDR⊗IAS	36.15±0.26[e]		579±224	1392±128

[a] Q value fitted at T_π=164 MeV.
[b] Q value fitted at T_π=164 MeV, fixed elsewhere.
[c] Q value fitted at T_π=293.7 MeV, fixed elsewhere.
[d] Q value fitted at T_π=230 MeV, fixed elsewhere.
[e] Q value and width fitted at T_π=293.7 MeV, fixed at T_π=230 MeV; Lorentzian folded with the elastic peak shape, Γ=5.1±1.1 MeV.

TABLE III. Comparison of previous and present DCX measurements for T_π = 294 MeV.

	Previous			Present		
State	$-Q$ (MeV)	$d\sigma/d\Omega$ (nb/sr)	Width (MeV)	$-Q$ (MeV)	$d\sigma/d\Omega$ (nb/sr)	Width (MeV)
$T_{2<}$	14.4	26±10[a]		14.21±0.19	10.3±4.6	0
$T_{3<}$	17.4	130±20[a]	1.4	17.50±0.07	64.5±9.1	0
DIAS	21.9	630±30[a]	0	21.95±0.02	511.7±21.5	0
IAS⊗GDR	35.8	1350±300[b]	5.8±1.0	36.15±0.26	1392±128	5.1±1.1

[a]Reference [1].
[b]Reference [12].

DIAS, three possible states above the DIAS appear to be suggested, as well as two just below. The summed spectra are shown in Fig. 1. Of the structure above the DIAS, only the peak labeled $T_{1>}$ could be identified with the same Q value in all three spectra. The other two $T_>$ states were no better than two standard deviation peaks in any of the three individual spectra; in addition, the Q values were offset from 300 to 400 keV among spectra. Thus it is uncertain if the structure denoted as $T_{2>}$ and $T_{3>}$ corresponds to discrete states. Attempts to fit with Lorentzians folded with the elastic peak shape yielded no improvement. All the measurements from the present experiment are listed in Table II. Present and previous measurements—when available—are compared in Table III. We note that although some additional peaks are suggested in the spectra of Figs. 3 and 4, their cross section is smaller than two standard deviations, and have therefore been omitted from Table II.

IV. RESULTS AND CONCLUSIONS

Cross sections for the various discrete states are plotted vs incident pion energy in Figs. 6 and 7. Four distinct energy behaviors can be identified. The g.s. and the state denoted as $T_{2<}$ start with the largest cross section at resonance (T_π=164 MeV), have a deep minimum at the intermediate energy of T_π=230 MeV, and come back far from the resonance at T_π=293.7 MeV. One state, $T_{1<}$, has an excitation function which falls monotonically with increasing beam energy. The states just below the DIAS, namely, $T_{3<}$ and $T_{4<}$, peak at the intermediate energy of T_π=230 MeV. The former, however, has a cross section at T_π=293.7 MeV not far from that at the peak, while the latter's cross section at 164 MeV is closer to the peak cross section. Finally, the states above the DIAS display a monotonically increasing excitation function, so far as one can deduce from the data, as a function of projectile energy.

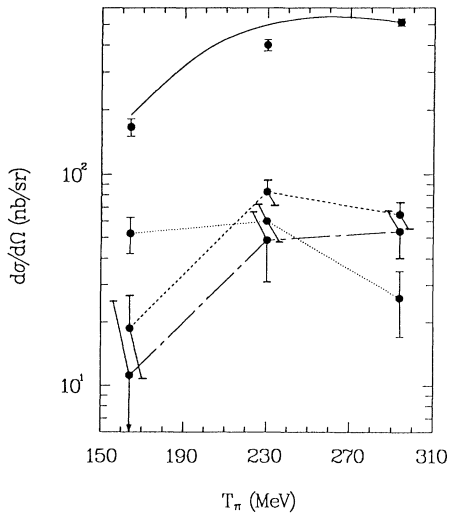

FIG. 6. Energy dependence of the cross sections for the states $T_{3<}$, $T_{4<}$, DIAS, and $T_{1>}$. The calculation (solid) is for the DIAS scaled to the data, as described in the text. The data points for the $T_{1>}$ (chain-dashes), $T_{3<}$ (dashes), and $T_{4<}$ (dots) are connected with lines to guide the eye.

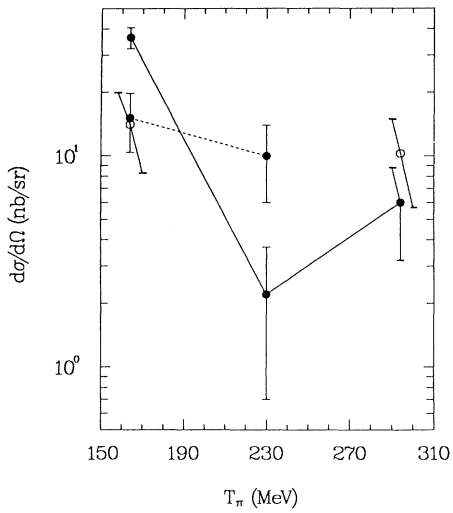

FIG. 7. As in Fig. 6, but for g.s., $T_{1<}$ (dashes), and $T_{2<}$ (solid) states. Note that the g.s. (open circles at 164 and 293.7 MeV) vanishes at 230 MeV. Also, $T_{1<}$ vanishes at 293.7 MeV.

The total cross section before subtraction of the background between the g.s. and the DIAS (exclusive) is highest at resonance (963 nb/sr) and it is relatively constant at higher beam energies (520 nb/sr at T_π=230 MeV and 526 nb/sr at T_π=293.7 MeV).

Meaningful microscopic calculations are presently not possible for DCX on ^{93}Nb; although the lowest-order sequential interaction can now be calculated quite accurately [13], precise shell-model calculations of the nuclear many-body wave functions for nuclei as heavy as ^{93}Nb are beyond the scope of the present work. As an illustration of a limited microscopic calculation which only displays the qualitative features of DCX on ^{93}Nb to the DIAS, we model the reaction ^{93}Nb$(\pi^+,\pi^-)^{93}$Tc with ^{92}Zr$(\pi^+,\pi^-)^{92}$Mo in the (severely restrictive) Gloeckner shell-model space. The calculation, obtained with the microscopic computer code $\mu\pi$ (named MICROPI) [13], is scaled to the DIAS data (Fig. 6). Recent, more realistic, microscopic sequential calculations which treat DCX as a two-step process [13] for lighter nuclei, however, have indicated that (a) several intermediate states reachable via single charge exchange (SCX) are comparable in strength to the isobaric analog state even for lighter nuclei, (b) several final states reachable via DCX are to be expected beyond the g.s. and the DIAS, and (c) the specific mechanism (i.e., non-spin-flip or spin-flip dominated process) in populating various DCX states depends largely on the nuclear structure of the target. As a general remark , one can state that—as we have established in the present experiment—several discrete states are expected to be reachable via DCX in heavy nuclei, and that no simple classification of these states is obvious. Rather, careful nuclear-structure analysis of the target is necessary in order to understand the nature of the mechanism(s) involved in populating them. Of the states which can be populated via DCX, only the DIAS can be expected to have common characteristics for all nuclei, as it is predominantly a sequential two-step process dominated by non-spin-flip amplitudes with $\Delta J = 0$.

With regard to the giant resonance mentioned earlier (Fig. 5), we ran the program $\mu\pi$ in the collective mode. In the calculations it was assumed that from the target nucleus the projectile scatters either to the IAS and subsequently via a giant dipole resonance to the GDR⊗IAS, or that the intermediate step involves the GDR with GDR⊗IAS as the final state. The assumptions are that the collective amplitudes for the protons and the neutrons are identical for the IAS, and of opposite sign for the GDR. With proton and neutron densities normalized to Z and N, respectively, these conditions translate into the requirement that the strength parameters β_p, β_n [14] are identical for the IAS and of opposite sign for the GDR.

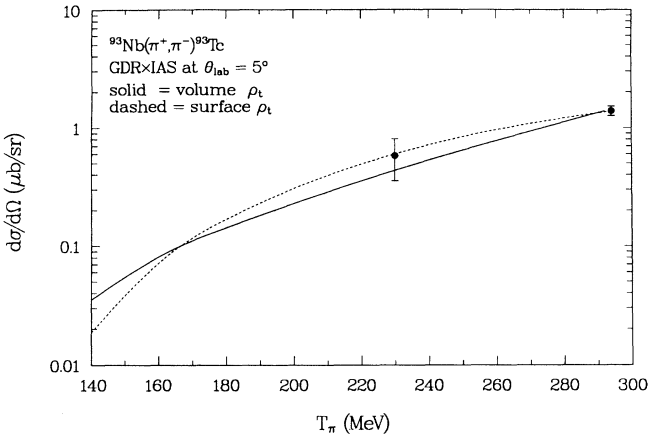

FIG. 8. As in Fig. 6, but for the GDR⊗IAS. Curves are from coupled-channel calculations described in text.

Two calculations with unit collective strengths β_p and β_n, and then scaled to the data at 294 MeV, are presented (Fig. 8). The first (solid) uses a volume density, identical to that of the ground state, for the IAS. The dashed curve uses a surface transition density, viz., the derivative of the g.s. density with the same geometrical parameters. Both calculations use a surface-derivative transition density for the GDR. We note that the observed energy dependence for the GDR⊗IAS cross section is consistent with the calculations.

In summary, we observe a number of states below the DIAS in DCX on ^{93}Nb. The cross sections exhibit different energy dependence. In particular, none of them have the same energy dependence as the DIAS.

ACKNOWLEDGMENTS

We thank J. M. O'Donnell for conversations and assistance. We acknowledge financial support from the National Science Foundation and the Department of Energy.

[1] C. F. Moore *et al.*, Phys. Rev. C **44**, 2209 (1991).
[2] P. A. Seidl *et al.*, Phys. Rev C **42**, 1929 (1990).
[3] J. M. O'Donnell, Phys. Rev. C **46**, 2259 (1992).
[4] R. A. Gilman *et al.*, Phys. Rev. C **35**, 1334 (1987).
[5] M. B. Johnson, E. R. Siciliano, H. Toki, and A. Wirzba, Phys. Rev. Lett. **52**, 593 (1984).
[6] R. A. Gilman, H. T. Fortune, M. B. Johnson, E. R. Siciliano, H. Toki, and A. Wirzba, Phys. Rev. C **32**, 349 (1985).
[7] A. Wirzba, H. Toki, E. R. Siciliano, M. B. Johnson, and R. Gilman, Phys. Rev. C **40**, 2745 (1989).
[8] R. A. Gilman, Ph.D. dissertation, University of Pennsylvania, 1985; Los Alamos Report No. LA-10524-T, 1985.
[9] Lampf Users Handbook, Clinton P. Anderson Meson Physics Facility, Report No. MP-DO-3-UHB (Rev.), 1984.
[10] H. A. Thiessen *et al.*, Los Alamos Report No. LA-6663-MS, 1977.
[11] D. Beatty *et al.*, experiment 1017.
[12] S. Mordechai *et al.*, Phys. Rev. C **40**, 850 (1989).
[13] M. A. Kagarlis, M. B. Johnson, and H. T. Fortune (in preparation).
[14] M. A. Kagarlis and H. T. Fortune, Phys. Rev. C **45**, 1351 (1992).